Atmos. Meas. Tech. Discuss., 8, 2851–2879, 2015
www.atmos-meas-tech-discuss.net/8/2851/2015/
doi:10.5194/amtd-8-2851-2015

Atmospheric Measurement Techniques Discussions
Open Access

Correcting aethalometer black carbon data for measurement artifacts by using inter-comparison methodology based on two different light attenuation increasing rates

Y.-H. Cheng and L.-S. Yang

Department of Safety, Health and Environmental Engineering, Ming Chi University of Technology, 84 Gungjuan Rd, Taishan, New Taipei 24301, Taiwan

Received: 10 February 2015 – Accepted: 5 March 2015 – Published: 17 March 2015

Correspondence to: Y.-H. Cheng (yhcheng@mail.mcut.edu.tw)

Published by Copernicus Publications on behalf of the European Geosciences Union.

Abstract

In black carbon (BC) measurements obtained using the filter-based optical technique, artifacts are a major problem. Recently, it has become possible to correct these artifacts to a certain extent by using numerical methods. Nevertheless, all correction schemes have their advantages and disadvantages under field conditions. In this study, a new correction model that can be used for determining artifact effects on BC measurements was proposed; the model is based on two different light attenuation (ATN) increasing rates. Two aethalometers were used to measure ATN values in parallel at aerosol sampling flow rates of 6 and 2 L min^{-1}. In the absence of sampling artifacts, the ratio of ATN values measured by the two aethalometers should be equal to the ratio of the sampling flow rates (or aerosol deposition rates) of these two aethalometers. In practice, the ratio of ATN values measured by the two aethalometers was not the same as the ratio of the sampling flow rates of the aethalometers because the aerosol loading effects varied with the aerosol deposition rate. If the true ATN value can be found, then BC measurements can be corrected for artifacts by using the true ATN change rate. Therefore, determining the true ATN value was the primary objective of this study. The proposed correction algorithm can be used to obtain the true ATN value from ATN values acquired at different sampling flow rates, and the actual BC mass concentrations can be determined from the true ATN change rate. Before BC correction, the BC concentration measured at the sampling flow rate of 6 L min^{-1} was smaller than that measured at 2 L min^{-1} by approximately 13 and 9 % in summer and winter seasons, respectively. After BC correction by using the true ATN value, the corrected BC for 6 L min^{-1} can be exactly equal to the corrected BC for 2 L min^{-1}. Field test results demonstrated that loading effects on BC measurements could be corrected accurately by using the proposed model. Additionally, the problem of enhanced light ATN caused by light scattering at the unloaded filter can be overcome without using any light scattering coefficient. Therefore, the correction algorithm can be applied to a newly designed instrument to determine actual real-time BC concentrations by using

AMTD
8, 2851–2879, 2015

two sampling spots for different aerosol deposition rates. Moreover, a simple empirical correction scheme for post-processing for correcting the existed aethalometer BC data is also presented. While this simple correction scheme is dependent on the aerosol type, it can be used to correct BC data when the primary source of BC and the weather conditions are similar to those in this study. Furthermore, two existed aethalometers with appropriate flow control can be used to create correction schemes suitable for different environments.

1 Introduction

Black carbon (BC) aerosols are produced by the incomplete combustion of carbonaceous fuels and are a crucial atmospheric constituent because of their potentially negative effects on climate and health (Ramanathan and Carmichael, 2008; Suglia et al., 2008; Jacobson, 2010; Power et al., 2011; Cornell et al., 2012; Bond et al., 2013). Hence, the measurement of BC has become increasingly crucial over the past decade in urban, rural, and background areas worldwide.

The most common method used to measure BC involves collecting aerosols on a filter and measuring the reduction in light transmission through the filter (Hansen et al., 1984). The aethalometer (AE; Magee Scientific) is one of the currently available devices used for measuring BC, and it is based on the filter-based optical technique. This device has been used extensively to monitor environmental BC mass concentrations because it can be operated easily and offers high time resolution (Watson et al., 2005; Park et al., 2006; Järvi et al., 2008; Chow et al., 2009; Cheng and Lin, 2013; Cheng et al., 2014). In the aethalometer, an air sample is drawn through a filter and aerosols are collected on the filter. Subsequently, the decrease in light transmission through the aerosols on the filter is measured. A decrease in the transmission implies increased attenuation (ATN). It is assumed that any ATN increase is solely due to light absorption by BC aerosols accumulated on the filter, and the BC concentration can therefore be calculated from the rate of ATN change. However, previous studies have shown that

AMTD
8, 2851–2879, 2015

the relationship between ATN change and BC concentration is not linear because of several reasons, one of which is that both light-scattering and light-absorbing particles collected on the filter alter the internal reflection properties of the filter (Liousse et al., 1993; Petzold et al., 1997; Reid et al., 1998; Bond et al., 1999; Weingartner et al., 2003). Measurement artifacts resulting from the nonlinearity of the aforementioned relationship have shown that because of the filter loading effect, the measured BC concentration decreases with an increase in the filter load, and the sample matrix effect causes scattering aerosols on the filter to increase the measured BC concentration.

Recently, it has become possible to correct these artifacts to a certain extent by using numerical methods (Weingartner et al., 2003; Arnott et al., 2005; Virkkula et al., 2007; Collaud Cone et al., 2010). Nevertheless, all correction methods have their advantages and disadvantages under field conditions. For example, although both aerosol scattering and absorption coefficients are considered in some of these correction methods, most BC measurements performed using the aethalometer in the field do not simultaneously acquire aerosol scattering coefficients, which are necessary for use in correction methods. Virkkula et al. (2007) proposed a simple procedure to correct the loading effects on aethalometer data without using the aerosol scattering coefficients. This procedure is based on the original measurement results of two continuous filter spots, and it is assumed that the BC concentration remains stable during the filter spot change and that the BC value measured with a lightly loaded filter is the closest to the real concentration value. A correction factor is then determined for each filter spot to correct the BC data. However, the assumption that the BC concentration is stable in the ambient environment during the filter spot change is not always true. Järvi et al. (2008) showed that the sensitivity of the correction factor with a difference value of 0.001 could cause an error of approximately 4 % in the BC concentrations when the correction model of Virkkula et al. (2007) is used. Moreover, the correction factor is not a constant value and is dependent on the density of the particles deposited on the filter.

Recently, a new generation aethalometer (AE33; Magee Scientific) based on a dual-spot method has been developed to obtain different particle deposition rates for differ-

AMTD
8, 2851–2879, 2015

ent sampling flow conditions (Drinovec et al., 2014). This dual-spot method involves a real-time model for determining the temporal variation of a compensation parameter for the loading effect. Cheng and Lin (2013) noted that different sets of ATN measurement results could differ significantly because of different aerosol deposition rates resulting from differences in the sampling flow rates or aerosol deposition areas among the used instruments. Therefore, a correction model for determining the artifacts on BC measurements based on different ATN increasing rates was developed in the current study. Two aethalometers were used to measure the ATN values at different aerosol sampling flow rates in parallel. In the absence of sampling artifacts, the ratio of the ATN values measured by these two aethalometers should be equal to the ratio of the sampling flow rates (or the aerosol deposition rates) of these two aethalometers. In practice, the ratio of the ATN values measured by these two aethalometers was not identical to the ratio of the sampling flow rates of these two aethalometers because of different aerosol loading effects resulting from different aerosol deposition rates. Hence, a simple algorithm, similar to the correction methods developed by Virkkula et al. (2007) and Drinovec et al. (2014), was used to determine the true ATN values. Field test results demonstrated that loading effects on BC measurements can be corrected accurately by using the proposed model. Moreover, the problem of enhanced light ATN because of light scattering at the unloaded filter can be overcome without using any light scattering coefficient. Field test results can also further provide users with a simple correction scheme during post-processing for correcting existing aethalometer BC data.

2 Methods

2.1 Correction model

For measuring BC with the filter-based optical technique, the optical ATN is defined as

$$\mathrm{ATN} = -100 \cdot \ln\left(\frac{I}{I_0}\right) \tag{1}$$

AMTD
8, 2851–2879, 2015

where I_0 and I are the intensities of light transmitted through a reference blank spot and a spot of aerosol on the filter, respectively. The factor 100 is introduced for convenience. The ATN change in a time interval (dATN/dt) is used to estimate the BC concentration as follows:

$$\mathrm{BC} = \frac{\mathrm{dATN}}{\mathrm{d}t} \cdot \frac{A}{Q} \cdot \frac{1}{\sigma_{\mathrm{ATN}}} \tag{2}$$

where A is the area of the sample spot, Q is the sampling flow rate, and σ_{ATN} is the black carbon optical mass cross section.

Drinovec et al. (2014) showed that the loading effect on BC can be corrected by using the following equation, which is similar to that proposed by Virkkula et al. (2007):

$$\mathrm{BC_c} = \frac{\mathrm{BC}}{(1 - k \cdot \mathrm{ATN})} \tag{3}$$

where $\mathrm{BC_c}$ and BC represent the corrected and measured black carbon concentration, respectively, and k is a correction factor. On the basis of the same principle as Eq. (2), the average BC ($\overline{\mathrm{BC}}$) from initial time t_0 ($t_0 = 0$) to time t can be expressed as

$$\overline{\mathrm{BC}} = \frac{\Delta\mathrm{ATN}}{\Delta t} \cdot \frac{A}{Q} \cdot \frac{1}{\sigma_{\mathrm{ATN}}} = \frac{\mathrm{ATN}}{t - t_0} \cdot \frac{A}{Q} \cdot \frac{1}{\sigma_{\mathrm{ATN}}} \tag{4}$$

Then, Eq. (3) can be written as

$$\mathrm{ATN_c} = \frac{\mathrm{ATN}}{(1 - k \cdot \mathrm{ATN})} \tag{5}$$

where $\mathrm{ATN_c}$ and ATN represent corrected and measured light ATN values, respectively.

In practice, if the true ATN value can be found, then the artifact effect on the BC measurement can be corrected from the true ATN change rate (dATN/dt). Therefore, determining the true ATN value was the main objective of this study. According to the

AMTD
8, 2851–2879, 2015

definition of light ATN, the ATN value is dependent on the amount of BC aerosol deposition. That is, different BC aerosol deposition rates can correspond to different ATN increasing rates. Nevertheless, the loading effect is a cumulative property of the cumulative deposit of aerosol on the filter, and it also directly influences the ATN measurement results. Therefore, different aerosol sampling flow rates in the same deposition area could lead to different loading effects on ATN measurement results.

According to Eq. (5), the ATN correction equation at different flow rates can be expressed as

$$\mathrm{ATN}_{\mathrm{F1,c}} = \frac{\mathrm{ATN}_{\mathrm{F1}}}{(1 - k \cdot \mathrm{ATN}_{\mathrm{F1}})} \tag{6}$$

$$\mathrm{ATN}_{\mathrm{F2,c}} = \frac{\mathrm{ATN}_{\mathrm{F2}}}{(1 - k \cdot \mathrm{ATN}_{\mathrm{F2}})} \tag{7}$$

where $\mathrm{ATN}_{\mathrm{F1}}$ and $\mathrm{ATN}_{\mathrm{F2}}$ represent the ATN measured at sampling flow rates Q_{F1} and Q_{F2}, respectively. In the absence of the artifact effect, the ratio of true ATN values measured at two different flow rates should be equal to the ratio of the two different sampling flow rates:

$$\frac{\mathrm{ATN}_{\mathrm{F2,c}}}{\mathrm{ATN}_{\mathrm{F1,c}}} = \frac{m_{\mathrm{BC,F2}}}{m_{\mathrm{BC,F1}}} = \frac{\mathrm{BC} \cdot Q_{\mathrm{F2}} \cdot t}{\mathrm{BC} \cdot Q_{\mathrm{F1}} \cdot t} = \frac{Q_{\mathrm{F2}}}{Q_{F1}} \tag{8}$$

where $m_{\mathrm{BC,F1}}$ and $m_{\mathrm{BC,F2}}$ represent the mass of black carbon aerosol deposited on the filter at sampling flow rates Q_{F1} and Q_{F2}, respectively.

In this model, the correction factor k is assumed to be fixed for an ATN/Q value. Then, k can be solved using Eqs. (6)–(8):

$$k = \frac{Q_{\mathrm{F1}} \cdot \mathrm{ATN}_{\mathrm{F2}} - Q_{\mathrm{F2}} \cdot \mathrm{ATN}_{\mathrm{F1}}}{Q_{\mathrm{F1}} \cdot \mathrm{ATN}_{\mathrm{F1}} \cdot \mathrm{ATN}_{\mathrm{F2}} - Q_{\mathrm{F2}} \cdot \mathrm{ATN}_{\mathrm{F1}} \cdot \mathrm{ATN}_{\mathrm{F2}}} \tag{9}$$

Therefore, the temporal variation of k can be determined on the basis of two measured ATN values for different sampling flow rates. Subsequently, the true ATN value can be

AMTD
8, 2851–2879, 2015

obtained from Eq. (5). Moreover, the actual BC concentration can be determined from the true ATN change rate by using Eq. (2).

2.2 Sampling equipment and data collection

In this study, BC (or ATN) was measured using two aethalometers (AE31; Magee Scientific); one aethalometer was operated at a sampling flow rate of $6\,\mathrm{L\,m^{-3}}$ (Q_{F6}), whereas the other was operated at a sampling flow rate of $2\,\mathrm{L\,m^{-3}}$ (Q_{F2}). The filter tape in these two aethalometers was shifted automatically to expose a pristine spot on the filter at the same time every eight hours to ensure that the two sampling spots had a fixed starting and ending time of the sampling for internal comparison. The internal timer and sampling flow rate of the aethalometer were checked every week. The sampling site was located on the campus of Ming Chi University of Technology at Taishan, New Taipei City, Taiwan. The main source of BC at this sampling site was traffic. Sometimes, wood combustion could be observed on the campus for waste wood disposal. During the sampling periods, the two aethalometers were positioned adjacent to each other in a sampling cabin and the inlets of both aethalometers were approximately 2 m above the ground level outside the sampling cabin. The aethalometers were operated between 21 December 2013, and 24 January 2014 (winter season), and between 5 July 2014, and 26 September 2014 (summer season). The logging interval for all measurements was set at 5 min. The filter tape used was a quartz material filter (Pallflex Q250F), which was suggested by the aethalometer manufacturer. To avoid water vapor condensing on the deposited aerosols in the summer season, a diffusion dryer with silica gel was installed on the sampling line. The silica gel was replaced every two days during sampling periods. When the diffusion dryer was not used, negative values could be observed in BC data sets at noon under conditions of high temperature and high relative humidity. Negative values were also recorded in BC data sets when sampling was performed at very low ambient concentrations at midnight and early morning hours, especially at low sampling flow rates. If negative values appeared in the data set of a sampling spot, the entire data for the sampling spot was excluded

AMTD
8, 2851–2879, 2015

from further treatment. Local meteorological data such as temperature and relative humidity were recorded using a Vantage Pro 2™ weather station (Davis Instruments). Table 1 shows the ambient temperature and relative humidity during the sampling periods. The average temperature during the summer season was significantly higher than that during the winter season by approximately 15 °C ($p < 0.001$). The average relative humidity did not differ significantly between the summer and the winter seasons ($p = 0.086$).

Before beginning field sampling, the performance of the two aethalometers was compared at the sampling site for two sampling flow rates, 6 and 2 L min^{-1}, for 2–3 days. The hourly measured results obtained using the two aethalometers are shown in Fig. 1. The hourly average BC mass concentrations in units of nanogram per cubic meter were calculated using 5 min raw data. Statistical results indicated that the intercepts were −30.751 (95 % confidence interval (CI): −56.091 to −5.411) and −18.119 (95 % CI: −43.841–7.603) for the sampling flow rates of 6 and 2 L min^{-1}, respectively, and the intercepts were not considerably different from zero ($p = 0.019$ for 6 L min^{-1} and $p = 0.163$ for 2 L min^{-1}). The slopes determined for these two flow rates were 0.991 (95 % CI: 0.985–0.997) and 0.988 (95 % CI: 0.980–0.997), respectively, and the slopes were significantly different from 1.0 ($p < 0.001$ for both). These comparison results indicated that the performance of both aethalometers used in this study could be considered to be similar to each other.

3 Results and discussion

3.1 ATN values and black carbon mass concentrations before and after correction

Figure 2 shows the relationships between ATN values for sampling flow rates of 6 and 2 L min^{-1} before and after correction in the summer and winter seasons. Before ATN correction, the ATN_{F6} value was smaller than the value of 3 × ATN_{F2}, indicating

AMTD
8, 2851–2879, 2015

the presence of the artifact effect on the ATN measurement result. When the ATN_{F6} value increased, it deviated considerably from the value of $3 \times ATN_{F2}$, especially for the 370 nm wavelength. The measurement results demonstrated that the loading effect on the ATN value at short wavelengths was stronger than that at long wavelengths. After ATN correction using Eqs. (6)–(9), the ratio of the ATN_{F6} value to the ATN_{F2} value could fall to 3 : 1. That is, the true ATN values could be determined using the algorithms proposed in this study. Subsequently, the actual BC mass concentration could be estimated from the true ATN change rate. Before BC correction, the measured BC_{F6} was significantly smaller than the measured BC_{F2} by approximately 13 and 9 % in the summer and winter seasons ($p < 0.001$ for both), respectively. After BC correction by using the true ATN value, the corrected BC_{F6} could be exactly equal to the corrected BC_{F2}. Figure 3 presents a comparison of BC corrected using the proposed model and that corrected using the correction model of Drinovec et al. (2014). The correction model of Drinovec et al. (2014) is presented in Eq. (3), and the correction factor in this model can be easily estimated from the following equation on the basis of the measurement results of BC and ATN at sampling flow rates of 6 and 2 L min^{-1}:

$$k = \frac{BC_{F2} - BC_{F6}}{BC_{F2} \cdot ATN_{F6} - BC_{F6} \cdot ATN_{F2}} \tag{10}$$

The corrected BC estimated using the model proposed in this study was comparable with that obtained using the correction model of Drinovec et al. (2014) ($p = 0.307$ for summer; $p = 0.915$ for winter). The k value estimated using the model of Drinovec et al. (2014) exhibited significant variations between negative and positive values for the entire data set. By contrast, the k value determined using the proposed model approached a constant value steadily when the ATN value increased. The steady variation of the k value in the proposed model was due to k being determined from a cumulative ATN value, rather than an instant differential ATN value.

AMTD
8, 2851–2879, 2015

3.2 Influence of light scattering behavior on unloaded filter

The relationship between measured ATN_{F6} and ATN_{F2} is shown in Fig. 2, and it can be expressed as a power law relationship through measurement data fitting. On the basis of analytical results, the relationship between k and ATN/Q could be determined using Eq. (9) and the relationship between measured ATN_{F6} and ATN_{F2}, as shown in Fig. 4. Analytical results showed that the relationship between k and ATN/Q for sampling flow rates of 6 and $2\,L\,min^{-1}$ was similar, especially for long wavelengths. This result indicated that the assumption of the k value being fixed for an ATN/Q value in the proposed model was reasonable. Analytical results indicated that the k value was negative at extremely small ATN/Q values. The k value increased rapidly as ATN/Q increased, and then approached a constant value. Weingartner et al. (2003) noted that multiple scattering in the nearly unloaded fiber filter could enhance light absorption. Therefore, a negative k value could be observed at small ATN/Q values, which was reasonable in terms of the light scattering behavior of the nearly unloaded filter at a new sampling spot, especially at short wavelengths in the winter season. In this study, it was found that with increasing aerosol load on the filter, the influence of the light scattering behavior of the filter matrix could be eliminated. When a sufficient amount of aerosol was sampled on the filter, k initially increased as a positive value and then decreased gradually and steadily to a constant value. These observation results indicated that the proposed model could overcome the problem of enhanced light ATN resulting from light scattering at a new sampling spot, without using any light scattering coefficient.

3.3 Absorption Ångström exponent and emission source of black carbon

The absorption Ångström exponent α can be used as an index to determine the type of BC emission sources (Sandradewi et al., 2008), and it is computed from the aerosol

AMTD
8, 2851–2879, 2015

light absorption between 470 and 950 nm wavelengths as follows:

$$\alpha = \frac{\ln\left(b_{\mathrm{abs},\lambda=470}/b_{\mathrm{abs},\lambda=950}\right)}{\ln\left(950/470\right)} \tag{11}$$

where $b_{\mathrm{abs},\lambda=470}$ and $b_{\mathrm{abs},\lambda=950}$ are the absorption coefficients of aerosol at 470 and 950 nm wavelengths, respectively. The absorption coefficient of aerosol can be determined from the change rate of ATN:

$$b_{\mathrm{abs}} = \frac{\mathrm{dATN}}{\mathrm{d}t} \cdot \frac{A}{Q} \cdot \frac{1}{C} \tag{12}$$

where C is a light enhancement parameter. It is associated with multiple scattering of the light beam at the filter fibers in the unloaded filter, and it is strongly dependent on the filter material (Weingartner et al., 2003). In this study, C was set as 2.14 for the quartz filter (Weingartner et al., 2003; Drinovec et al., 2014).

Kirchstetter and Novakov (2004) noted that the absorption Ångström exponent value ranged between 0.8 and 1.1 for diesel soot. Day et al. (2006) showed that the absorption Ångström exponent values were between 0.9 and 2.2 for fresh wood smoke aerosol, which strongly depended on the type of wood and burning conditions. Sandradewi et al. (2008) also demonstrated that the absorption Ångström exponent values were 1.1 and 1.8–1.9 for traffic and wood burning, respectively. A high absorption Ångström exponent value could be observed for wood combustion aerosol that is due to the compounds of the aerosol with strong absorption in the UV. However, the filter loading effect also strongly influences the calculation of the absorption Ångström exponent value. Table 2 shows the absorption Ångström exponent values calculated from measured $\mathrm{ATN}_{\mathrm{F6}}$ and $\mathrm{ATN}_{\mathrm{F2}}$ and from corrected ATN in the summer and winter seasons. Analytical results showed that the absorption Ångström exponent value could be improved from 1.01 ± 0.22 (estimated from measured $\mathrm{ATN}_{\mathrm{F6}}$) and 1.11 ± 0.33 (estimated from measured $\mathrm{ATN}_{\mathrm{F2}}$) to 1.17 ± 0.44 (estimated from corrected ATN) in the summer

AMTD
8, 2851–2879, 2015

season. In the winter season, the absorption Ångström exponent value could be increased from 1.01 ± 0.18 (estimated from measured ATN_{F6}) and 1.10 ± 0.20 (estimated from measured ATN_{F2}) to 1.15 ± 0.24 (estimated from corrected ATN). The absorption Ångström exponent values computed using the ATN measured at the sampling flow rates of 6 and 2 $L\,min^{-1}$ were relatively lower than those estimated from the corrected ATN ($p < 0.001$ for both), indicating that the absorption Ångström exponent value could be significantly underestimated because of the filter loading effect. According to the estimated absorption Ångström exponent values, the primary emission source of BC at the sampling site was traffic.

3.4 Simple correction scheme for post-processing for correcting black carbon data

Despite the negative k value for small ATN/Q, the k value showed a power law relationship with ATN/Q for $ATN/Q > 3$ and 10 in the summer and winter seasons, respectively (Fig. 5). Analytical results indicated that the k values could be predicted using the empirical equations presented in Table 3. Furthermore, the existed data sets of aethalometer AE31 could be post-corrected using these empirical equations for different sampling flow rates. First, the ATN values in existed data sets of aethalometer AE31 were divided by the sampling flow rate, and k was then estimated using the proposed empirical equations in Table 3. Second, the corrected ATN was determined from Eq. (5) by using the determined k and measured ATN. Finally, the corrected BC could be estimated from the change rate of the corrected ATN. It should be noted that the light scattering effect on the unloaded filer was neglected in the post-processing model.

Figure 6 shows the relationship between $(1 - k \times ATN)$ and ATN at different sampling flow rates. Analytical results showed that the value of $(1 - k \times ATN)$ was significantly affected by the ATN and sampling flow rate. When the ATN was very small, the value of $(1 - k \times ATN)$ approached 1.0. For different sampling flow rates, the $(1 - k \times ATN)$ value differed significantly for the same ATN conditions because of different aerosol deposition rates, indicating that the aerosol deposition density on the filter could influence the

AMTD
8, 2851–2879, 2015

extent of the aerosol loading effect on BC measurement results. Moreover, the aerosol loading effect on BC measurement results in the summer season was greater than that in the winter season by approximately 1–6 %, and it depended on the sampling flow rate. This difference between seasons could be because of differences in the composition, source, and age of aerosols, in addition to the different weather conditions.

Figure 7 presents the results of a comparison between 5 min BC concentrations measured at sampling flow rates of 6 and 2 L min^{-1} before and after correction. The BC was corrected using the proposed post-processing model. Results showed that the corrected BC_{F6} mass concentrations were not significantly different from the corrected BC_{F2} mass concentrations ($p = 0.734$ for summer; $p = 0.594$ for winter), indicating that the post-processing model could be effectively used to correct BC data for the loading effect.

3.5 Comparison with a previous correction model

Figure 8 presents the results of a comparison of BC corrected using the proposed post-processing model and the correction model of Weingartner et al. (2003). The correction model developed by Weingartner et al. (2003) is widely used to correct BC data on the basis of the measured ATN value, and it can be expressed as

$$BC_c = \frac{BC}{R(ATN)} \tag{13}$$

$$R(ATN) = \left(\frac{1}{f} - 1\right)\frac{\ln(ATN) - \ln(10)}{\ln(50) - \ln(10)} + 1 \tag{14}$$

where f is a fit parameter dependent on the aerosol type. BC corrected using the post-processing model was comparable with that corrected using the correction model of Weingartner et al. (2003) for $f = 1.21$ and 1.14 in the summer and winter seasons, respectively, at the sampling flow rate of 6 L min^{-1}. For the sampling flow rate of 2 L min^{-1}, BC corrected using the post-processing model was comparable with that

AMTD
8, 2851–2879, 2015

corrected using the correction model of Weingartner et al. (2003) for $f = 1.25$ and 1.15 in the summer and winter seasons, respectively. However, BC corrected using the post-processing model was slightly higher than that corrected using the correction model of Weingartner et al. (2003) ($p \leq 0.019$), except for the sampling flow rate of 6 L min^{-1} in the winter season ($p = 0.123$). BC corrected using the correction model of Weingartner et al. (2003) was significantly lower than that corrected using the post-processing model when ATN was small, and this is possibly because the function R(ATN) in the correction model of Weingartner et al. (2003) was larger than 1.0 for ATN < 10. In other words, the corrected BC was smaller than that corrected using the post-processing model for R(ATN) > 1.0. Otherwise, the BC corrected using the correction model of Weingartner et al. (2003) was higher than that corrected using the post-processing model for ATN > 20, especially for ATN > 50. Moreover, the parameter f in the correction model of Weingartner et al. (2003) is significantly dependent on the aerosol type, and it was difficult to determine from field sampling data.

4 Conclusions

This study developed a new method based on two different light ATN increasing rates to improve the measurement of aerosol black carbon. The proposed correction model can overcome the light scattering effect and aerosol loading effect on BC measurement results simultaneously, and it can be used in a newly designed instrument to determine the actual BC concentration in real time by using two sampling spots under different aerosol deposition rates. Moreover, this study provided a simple empirical correction scheme for post-processing for correcting the existed aethalometer BC data. Although this simple correction scheme is dependent on the aerosol type, it can be used to correct BC data when the primary source of BC and the weather conditions are similar to those in this study. Moreover, two existed aethalometers under appropriate flow control can be used to create correction schemes for different environments.

AMTD
8, 2851–2879, 2015

Acknowledgements. The authors would like to thank the Ministry of Science and Technology of the Republic of China, Taiwan, for financially supporting this research under Contract No. MOST 102-2221-E-131-002-MY3.

References

Arnott, W. P., Hamasha, K., Moosmüller, H., Sheridan, P. J., and Ogren, J. A.: Towards aerosol light-absorption measurements with a 7-wavelength aethalometer: evaluation with a photoacoustic instrument and 3-wavelength nephelometer, Aerosol Sci. Tech., 39, 17–29, 2005.

Bond, T. C., Anderson, T. L., and Campbell, D.: Calibration and intercomparison of filter-based measurements of visible light absorption by aerosols, Aerosol Sci. Tech., 30, 582–600, 1999.

Bond, T. C., Doherty, S. J., Fahey, D. W., Forster, P. M., Berntsen, T., DeAngelo, B. J., Flanner, M. G., Ghan, S., Karcher, B., Koch, D., Kinne, S., Kondo, Y., Quinn, P. K., Sarofim, M. C., Schultz, M. G., Schulz, M., Venkataraman, C., Zhang, H., Zhang, S., Bellouin, N., Guttikunda, S. K., Hopke, P. K., Jacobson, M. Z., Kaiser, J. W., Klimont, Z., Lohmann, U., Schwarz, J. P., Shindell, D., Storelvmo, T., Warren, S. G., and Zender, C. S.: Bounding the role of black carbon in the climate system: a scientific assessment, J. Geophys. Res.-Atmos., 118, 5380–5552, 2013.

Cheng, Y. H. and Lin, M. H.: Real-time performance of the microAeth® AE51 and the effects of aerosol loading on its measurement results at a traffic site, Aerosol Air Qual. Res., 13, 1853–1863, 2013.

Cheng, Y. H., Liao, C. W., Liu, Z. S., Tsai, C. J., and Hsi, H. C.: A size-segregation method for monitoring the diurnal characteristics of atmospheric black carbon size distribution at urban traffic sites, Atmos. Environ., 90, 78–86, 2014.

Chow, J. C., Watson, J. G., Doraiswamy, P., Chen, L. W. A., Sodeman, D. A., Lowenthal, D. H., Park, K., Arnott, W. P., and Motallebi, N.: Aerosol light absorption, black carbon, and elemental carbon at the Fresno Supersite, California, Atmos. Res., 93, 874–887, 2009.

Collaud Coen, M., Weingartner, E., Apituley, A., Ceburnis, D., Fierz-Schmidhauser, R., Flentje, H., Henzing, J. S., Jennings, S. G., Moerman, M., Petzold, A., Schmid, O., and Baltensperger, U.: Minimizing light absorption measurement artifacts of the aethalometer: evaluation of five correction algorithms, Atmos. Meas. Tech., 3, 457–474, doi:10.5194/amt-3-457-2010, 2010.

AMTD
8, 2851–2879, 2015

Cornell, A. G., Chillrud, S. N., Mellins, R. B., Acosta, L. M., Miller, R. L., Quinn, J. W., Yan, B., Divjan, A., Olmedo, d. O. E., Lopez-Pintado, S., Kinney, P. L., Perera, F. P., Jacobson, J. S., Goldstein, I. F., Rundle, A. G., and Perzanowski, M. S.: Domestic airborne black carbon and exhaled nitric oxide in children in NYC, J. Expo. Sci. Env. Epid., 22, 258–266, 2012.

Day, D. E., Hand, J. L., Carrico, C. M., Engling, G., and Malm, W. C.: Humidification factors from laboratory studies of fresh smoke from biomass fuels, J. Geophys. Res., 111, D22202, 2006.

Drinovec, L., Močnik, G., Zotter, P., Prévôt, A. S. H., Ruckstuhl, C., Coz, E., Rupakheti, M., Sciare, J., Müller, T., Wiedensohler, A., and Hansen, A. D. A.: The "dual-spot" aethalometer: an improved measurement of aerosol black carbon with real-time loading compensation, Atmos. Meas. Tech. Discuss., 7, 10179–10220, doi:10.5194/amtd-7-10179-2014, 2014.

Hansen, A. D. A., Rosen, H., and Novakov, T.: The aethalometer – an instrument for the real-time measurement of optical absorption by aerosol particles, Sci. Total Environ., 36, 191–196, 1984.

Jacobson, M. Z.: Short-term effects of controlling fossil-fuel soot, biofuel soot and gases, and methane on climate, Arctic ice, and air pollution health, J. Geophys. Res., 115, D114209, doi:10.1029/2009JD013795, 2010.

Järvi, L., Junninen, H., Karppinen, A., Hillamo, R., Virkkula, A., Mäkelä, T., Pakkanen, T., and Kulmala, M.: Temporal variations in black carbon concentrations with different time scales in Helsinki during 1996–2005, Atmos. Chem. Phys., 8, 1017–1027, doi:10.5194/acp-8-1017-2008, 2008.

Kirchstetter, T. W. and Novakov, T.: Evidence that the spectral dependence of light absorption by aerosols is affected by organic carbon, J. Geophys. Res., 109, D21208, 2004.

Liousse, C., Cachier, H., and Jennings, S. G.: Optical and thermal measurements of black carbon aerosol content in different environments: variation of the specific attenuation cross-section, sigma, Atmos. Environ., 27, 1203–1211, 1993.

Park, K., Chow, J. C., Watson, J. G., Trimble, D. L., Doraiswamy, P., Arnott, W. P., Stroud, K. R., Bowers, K., Bode, R., Petzold, A., and Hansen, A. D. A.: Comparison of continuous and filter-based carbon measurements at the Fresno Supersite, J. Air Waste Manage., 56, 474–491, 2006.

Petzold, A., Kopp, C., and Niessner, R.: The dependence of the specific attenuation cross-section on black carbon mass fraction and particle size, Atmos. Environ., 31, 661–672, 1997.

AMTD
8, 2851–2879, 2015

Correcting aethalometer BC data for measurement artifacts

Y.-H. Cheng and L.-S. Yang

Power, M. C., Weisskopf, M. G., Alexeeff, S. E., Coull, B. A., Spiro., A., and Schwartz, J.: Traffic-related air pollution and cognitive function in a cohort of older men, Environ. Health Persp., 119, 682–687, 2011.
Ramanathan, V. and Carmichael, G.: Global and regional climate changes due to black carbon, Nat. Geosci., 1, 221–227, 2008.
Reid, J. S., Hobbs, P. V., Liousse, C., Vanderlei Martins, J., Weiss, R. E., and Eck, T. F.: Comparisons of techniques for measuring shortwave absorption and black carbon content of aerosols from biomass burning in Brazil, J. Geophys. Res., 103, 32031–32040, 1998.
Sandradewi, J., Prévôt, A. S. H., Szidat, S., Perron, N., Alfarra, M. R., Lanz, V. A., Weingartner, E., and Baltensperger, U.: Using aerosol light absorption measurements for the quantitative determination of wood burning and traffic emission contributions to particulate matter, Environ. Sci. Technol., 42, 3316–3323, 2008.
Suglia, S. F., Gryparis, A., Schwartz, J., and Wright, R. J.: Association between traffic-related black carbon exposure and lung function among urban women, Environ. Health Persp., 116, 1333–1337, 2008.
Virkkula, A., Mäkelä, T., Hillamo, R., Yli-Tuomi, T., Hirsikko, A., Hämeri, K., and Koponen, I. K.: A simple procedure for correcting loading effects of aethalometer data, J. Air Waste Manage., 57, 1214–1222, 2007.
Watson, J. G., Chow, J. C., and Chen, L. W. A.: Summary of organic and elemental carbon/black carbon analysis methods and intercomparisons, Aerosol Air Qual. Res., 5, 65–102, 2005.
Weingartner, E., Saathoff, H., Schnaiter, M., Streit, N., Bitnar, B., and Baltensperger, U.: Absorption of light by soot particles: determination of the absorption coefficient by means of aethalometers, J. Aerosol Sci., 34, 1445–1463, 2003.

AMTD
8, 2851–2879, 2015

Table 1. Ambient temperature and relative humidity during the sampling periods.

Season	Temperature, ˚C		Relative Humidity, %	
	Average ± SD	Min–Max	Average ± SD	Min–Max
Summer	32 ± 3	25–39	68 ± 13	37–93
Winter	17 ± 3	10–28	69 ± 14	34–91

AMTD
8, 2851–2879, 2015

Table 2. Absorption Ångström exponent values in the summer and winter seasons.

Season	Ångström exponent estimated from		
	measured ATN_{F6}	measured ATN_{F2}	corrected ATN
Summer	1.01 ± 0.22	1.11 ± 0.33	1.17 ± 0.44
Winter	1.01 ± 0.18	1.10 ± 0.20	1.15 ± 0.24

Average ± SD

AMTD
8, 2851–2879, 2015

Table 3. Parameters of empirical equations used for predicting the k values.

Season	Wavelength λ	$k = a \times \left(\frac{\mathrm{ATN}}{Q}\right)^b$	
		a	b
Summer	370 nm	0.0263	−0.8383
	470 nm	0.0168	−0.7602
	520 nm	0.0167	−0.8127
	590 nm	0.0149	−0.7843
	660 nm	0.0132	−0.7491
	880 nm	0.0149	−0.8099
	950 nm	0.0148	−0.8569
Winter	370 nm	0.0088	−0.5664
	470 nm	0.0100	−0.6623
	520 nm	0.0092	−0.6768
	590 nm	0.0089	−0.6835
	660 nm	0.0087	−0.6968
	880 nm	0.0087	−0.7532
	950 nm	0.0101	−0.8370

AMTD
8, 2851–2879, 2015

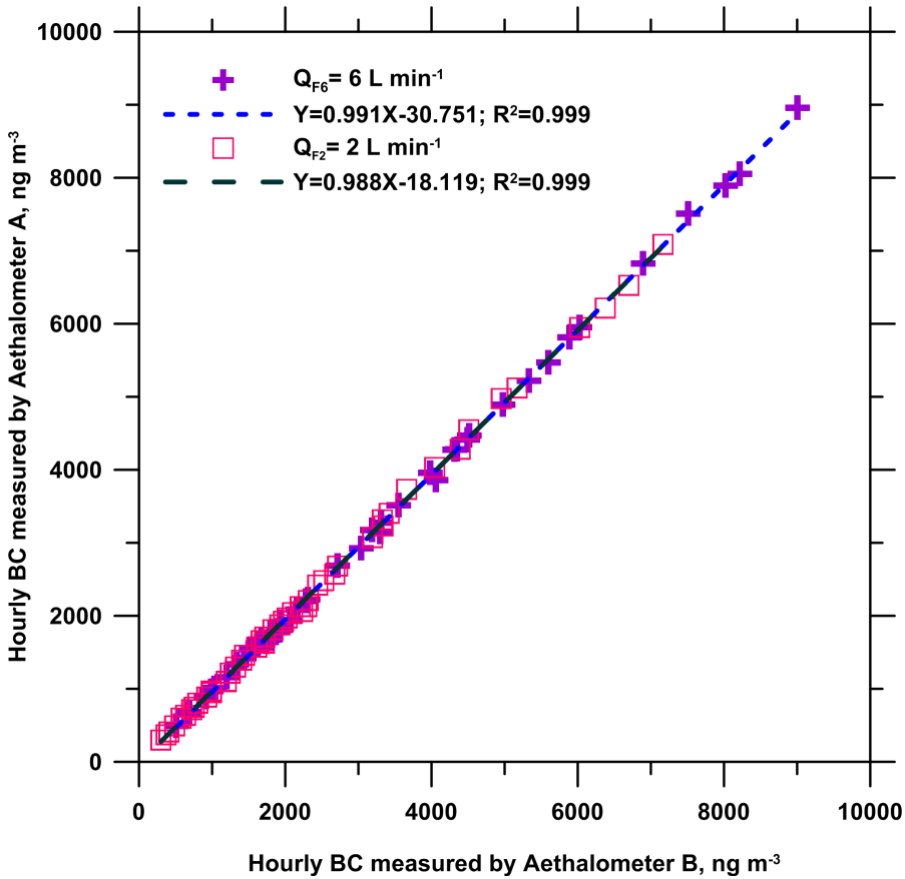

Figure 1. Comparison of hourly BC mass concentration measurements obtained with the two aethalometers used in this study.

AMTD
8, 2851–2879, 2015

Correcting aethalometer BC data for measurement artifacts

Y.-H. Cheng and L.-S. Yang

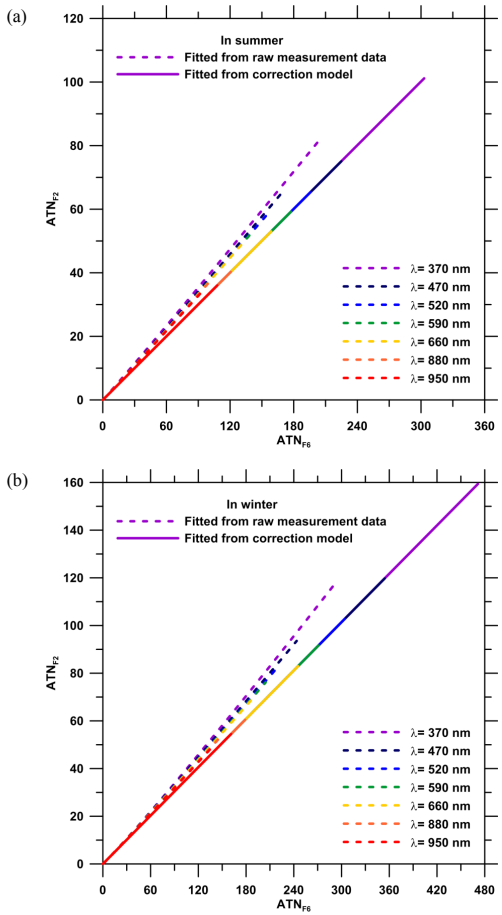

Figure 2. Relationship between ATN values for sampling flow rates of 6 and 2 L min^{-1} before and after correction for the **(a)** summer season and **(b)** winter season.

AMTD
8, 2851–2879, 2015

Correcting aethalometer BC data for measurement artifacts

Y.-H. Cheng and L.-S. Yang

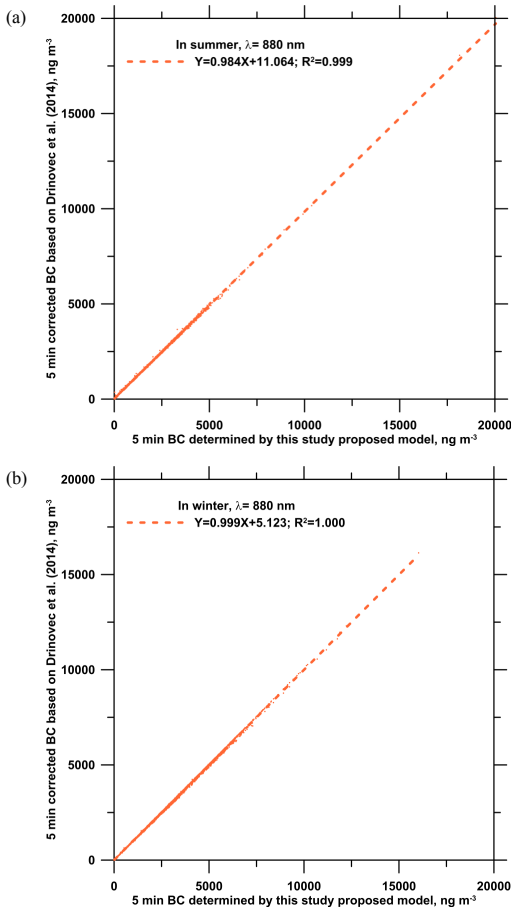

Figure 3. Comparison of BC corrected using the proposed model with that corrected using the correction model of Drinovec et al. (2014) for the **(a)** summer season and **(b)** winter season.

AMTD
8, 2851–2879, 2015

Correcting aethalometer BC data for measurement artifacts

Y.-H. Cheng and L.-S. Yang

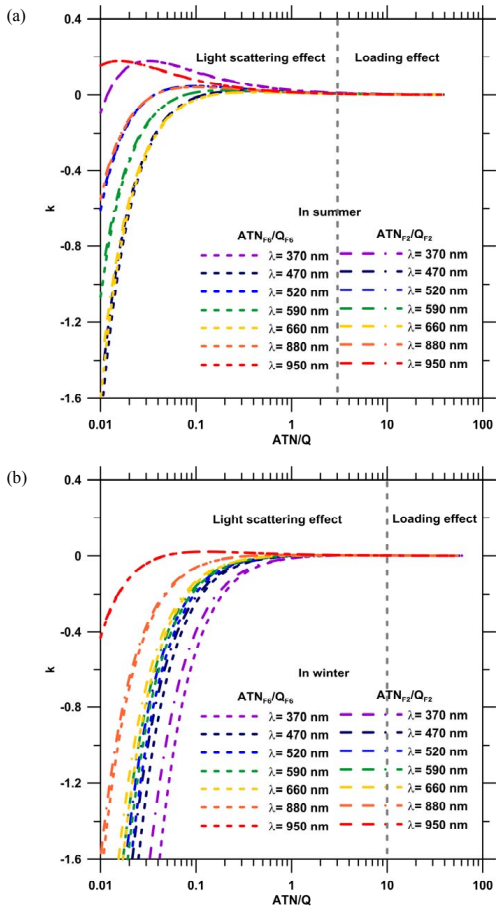

Figure 4. Relationships between k and ATN/Q for the **(a)** summer season and **(b)** winter season.

AMTD
8, 2851–2879, 2015

Correcting aethalometer BC data for measurement artifacts

Y.-H. Cheng and L.-S. Yang

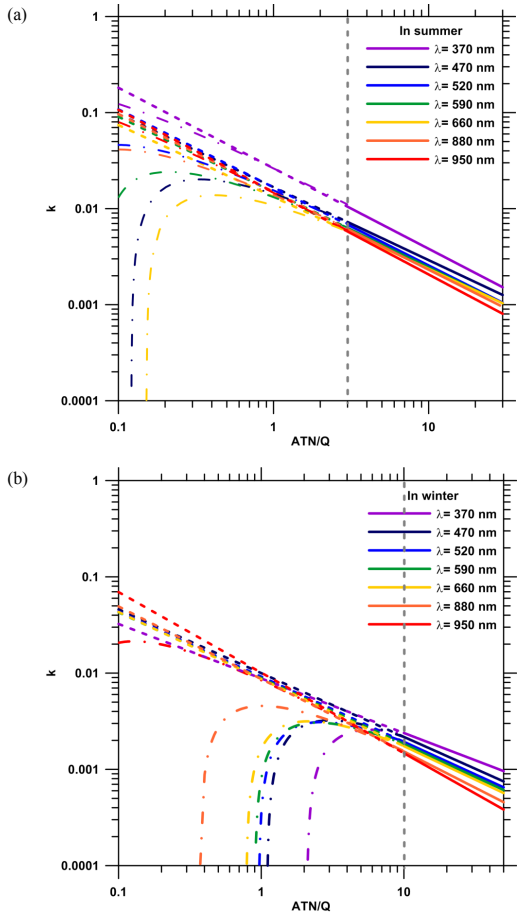

Figure 5. Power law relationship between k and ATN/Q **(a)** when ATN/$Q > 3$ in the summer season and **(b)** when ATN/$Q > 10$ in the winter season.

AMTD
8, 2851–2879, 2015

Correcting aethalometer BC data for measurement artifacts

Y.-H. Cheng and L.-S. Yang

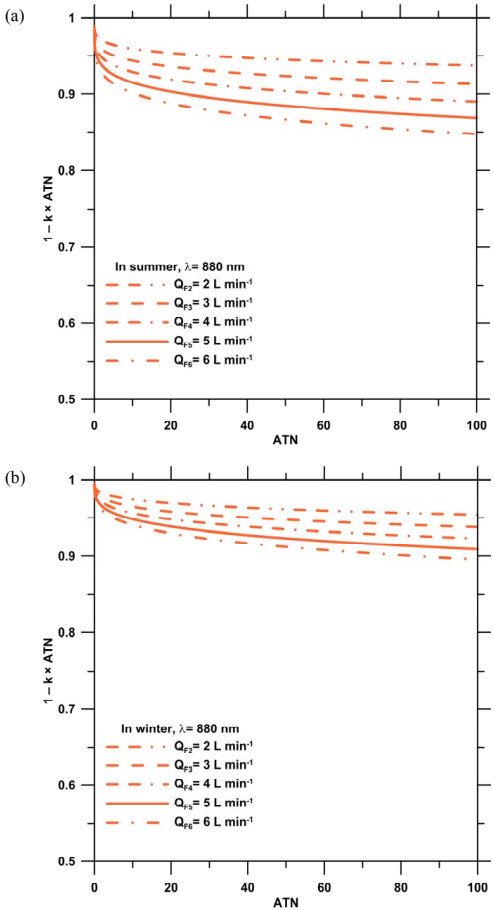

Figure 6. Relationship between (1 – k × ATN) and ATN at different sampling flow rates in the **(a)** summer season and **(b)** winter season.

AMTD
8, 2851–2879, 2015

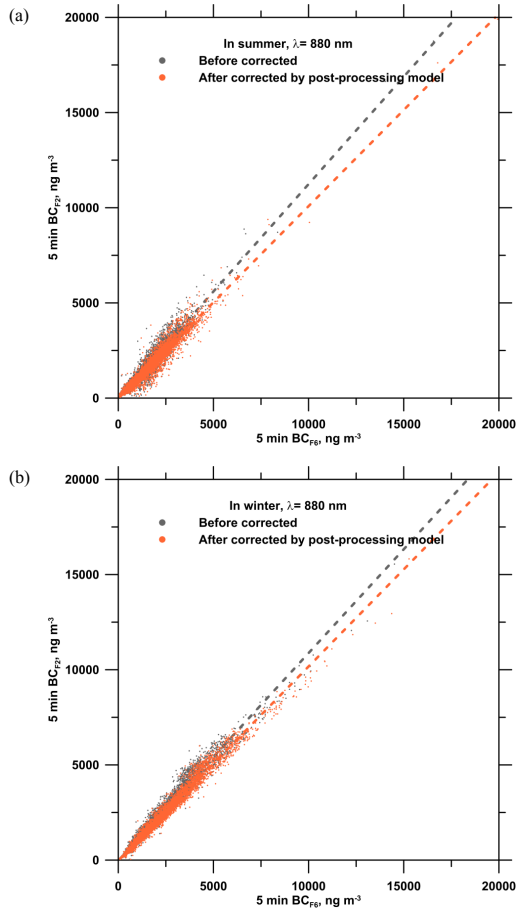

Figure 7. Comparison of the 5 min BC mass concentrations measured at sampling flow rates of 6 and 2 L min^{-1} before and after correction for the **(a)** summer season and **(b)** winter season.

AMTD
8, 2851–2879, 2015

Correcting aethalometer BC data for measurement artifacts

Y.-H. Cheng and L.-S. Yang

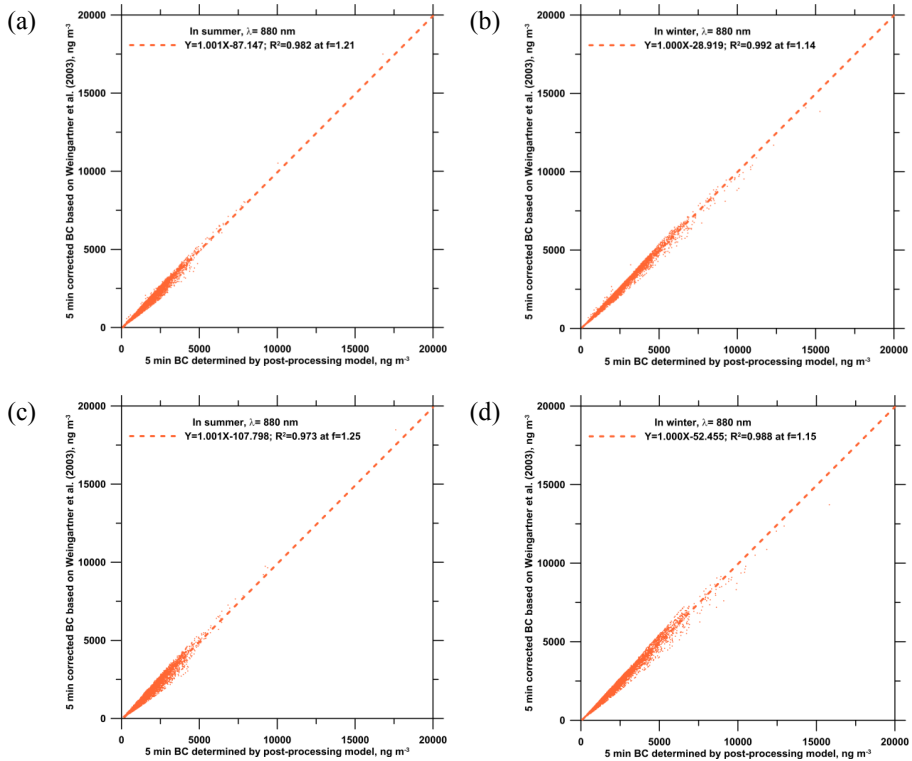

Figure 8. Comparison of the corrected BC obtained using the proposed postprocessing model with that obtained using the correction model of Weingartner et al. (2003) for sampling flow rates of **(a)** 6 L min^{-1} in the summer season, **(b)** 6 L min^{-1} in the winter season, **(c)** 2 L min^{-1} in the summer season, and **(d)** 2 L min^{-1} in the winter season.

AMTD
8, 2851–2879, 2015